# Effects of fuel/air mixture distribution on end-gas autoignition and pressure wave generations in knocking combustion

Tomonari Satoh, Hiroshi Terashima, Nobuyuki Oshima
School of engineering, Hokkaido University
Sapporo, Hokkaido, Japan

## 1 Introduction

Knocking in spark ignition gasoline engines is known as one of abnormal combustion associated with severe pressure oscillations. Knocking phenomenon is caused by autoignition of the end-gas formed between a propagating flame by spark ignition and an engine wall. The rapid heat release by the end-gas autoignition may lead to the generation of stronger pressure waves, which has a considerable potential to develop shock waves and eventually detonation waves. Such risks of knocking have been a large impediment of increasing compression ratio and thermal efficiency due to the occurrence of serious damage for engine components such as a piston head [1].

End-gas autoignition and a process of generating pressure waves are very rapid and small-scale phenomena. Therefore, despite a lot of researches concerning knocking combustion have been long conducted experimentally and numerically, detailed mechanisms of knocking still remain unclear. In recent years, numerical analyses using detailed reaction mechanisms have been carried out on addressing mechanisms of end-gas autoignition and pressure wave generations. For example, Gu at el. [2] identified five modes of flame propagation from a hot spot in a one-dimensional reactor. Dai at el. [3] studied flame propagation modes from a cool spot using *n*-heptane/air mixture.

The present study is sequel to our previous study [4], in which the mechanisms for the generation of strong pressure waves are discussed with the stoichiometric condition of *n*-heptane/air mixture. In a view of engine control, fuel injection is a controllable parameter and flexible control is possible for distributions of fuel/air mixtures in combustion chamber, which may have a great potential for reducing or suppressing knocking phenomena. However, there have been less studies concerning effects of fuel/air mixture distributions on knocking phenomena in past relevant literatures. Thus, the purpose of this paper is to numerically investigate the effects of fuel/air mixture distributions on knocking phenomena. The influence of equivalence ratio with a uniform distribution is first shown and the results of fuel/air mixture distributions are discussed. The compressible Navier-Stokes equations with a detailed chemical kinetics of *n*-heptane are applied to knocking combustion modeled in a one-dimensional constant volume reactor.

Correspondence to: tomonari-sato@eis.hokudai.ac.jp 

## 2 Numerical Methods

The governing equations are the compressible Navier-Stokes equations and the thermally perfect gas equation of state. An operator-splitting method is applied to the Navier-Stokes equations. The Navier-Stokes equations are solved under the condition that the chemical reaction is frozen, while the chemical reaction equations are solved under the constant volume and internal energy conditions. The production rate of chemical species is modeled with the Arrhenius equation and a detailed reaction mechanism. The updated variables in the Navier-Stokes equations and the chemical reaction equations are exchanged at each time step. A complete description for the numerical models and methods used here can be found in our previous paper [4].

## 3 Computational model and conditions

In this research, knocking combustion is modeled using a one-dimensional constant volume reactor as shown in Fig. 1. The length of the reactor is $L = 4.0$ cm. The symmetric condition is imposed on the left boundary and the right boundary is adiabatic wall. A flat hot kernel of 1400 K with a length of 1 mm is introduced at the left boundary in order to induce flame propagation. An end-gas region is then formed between the propagating flame and the adiabatic wall. Autoignition may occur in the end-gas region along with pressure and temperature increase in the reactor due to the flame propagation, followed by pressure wave generations. The present study investigates the effects of fuel/air mixture distributions on knocking combustion based on our previous study [4]. Figure 2 shows five initial conditions of fuel/air mixture distributions considered in this study. In uniform cases, three uniform distributions with the equivalence ratio of $\phi = 0.8$, $\phi = 1.0$ and $\phi = 1.2$ are used. The uniform case with $\phi = 1.0$ is named Case A for the following explanation. In the case of non-uniform distributions, two cases are considered as shown in Fig. 2. The first one is that the initial mixture consists of a rich mixture with $\phi = 1.2$ in the left region and a lean one with $\phi = 0.8$ in the right region (named Case B), assuming a condition, e.g., one that a rich mixture is distributed near a spark device. The other one is a case (named Case C) in which the opposite distribution for Case B is used for comparison.

The initial pressure is 5 atm in all the cases. The initial temperature parametrically changes from 550 to 850 K in order to investigate the influence of initial temperature. *n*-heptane/air mixture is considered for a working fluid. A uniform gird with a grid spacing of approximately 22 $\mu$m is used to resolve the flow fields. A grid dependency is preliminarily investigated in terms of a knocking intensity, demonstrating a grid converged solution with the present grid resolution.

A detailed reaction mechanism for *n*-heptane generated by a software of KUCRS [5], is applied in this study, which consist of 373 species and 1071 reactions. Figure 3 shows ignition delay times against initial temperatures for *n*-heptane/air mixtures at 5 atm for three equivalent ratios of $\phi = 0.8, 1.0, \text{and } 1.2$. The ignition delay time becomes smaller with increasing the equivalence ratio, which is observed in the region between 700 and 1100 K, while the overall trend with NTC characteristics is similar for all the conditions.

## 4 Results and discussions

Figure 4 shows the time history of pressure at the wall ($x = 4.0$ cm) for uniform cases. The pressure gradually increases due to the flame propagation in the constant volume reactor, and rapidly increases with the occurrence of end-gas autoignition. The pressure then continuously oscillates and eventually reach a

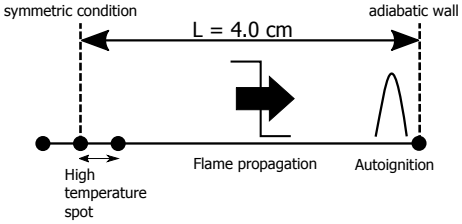


Figure 1: Schematic of a one-dimensional reactor

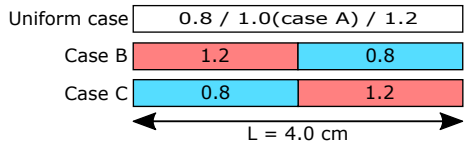


Figure 2: Initial condition of equivalence ratio

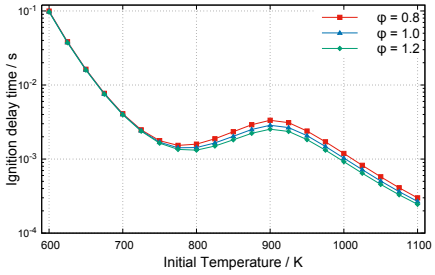


Figure 3: Ignition delay time of *n*-heptane in constant reactor

constant value. In the uniform case, the time of autoignition is shorter as the equivalence ratio increases.

Figure 5 presents the knocking intensity against initial temperature in uniform cases. In this study, the knocking intensity is defined with $p_{max}/p_e$ where $p_{max}$ is the first peak of the *maximum* pressure history in the reactor (e.g., not at the wall) and $p_e$ is the equilibrium pressure. A large peak of the knocking intensity appears at an initial temperature of 650 K for all the cases; refer to our previous research [4] on the generation mechanism of the large peak. In those cases, the knocking intensities are larger as the equivalence ratio increase.

Figure 6 shows the time history of pressure at the wall ($x = 4.0$ cm) for non-uniform cases with case A. It is found in the time histories that there is only one large peak of pressure in Case C such as uniform cases, whereas interestingly there exist two peaks in Case B: one is smaller at around $t = 7.5 \times 10^{-3}$ s and the other is larger at around $t = 8.1 \times 10^{-3}$ s. A cause for the appearance of two praks in Case B will be described later.

Figure 7 presents the knocking intensity against initial temperature in case A, case B and case C. The knocking intensity values obtained in Case C are almost like those in Case A (uniform case $\phi = 1.0$). On the other hand, the knocking intensity in Case B shows the largest values in all cases including uniform cases at around initial temperatures of 650 and 700 K which may be relevant to the two peaks in the pressure and temperature time histories.

Figures 8, 9, 11 and 12 show a detailed sequential profile of temperature and pressure at an initial temperature of 650 K for Case A, Case B and Case C. The results of Case A shown in Fig. 8 shows that end-gas autoignition first occur locally at the right wall (see profile 3), and a pressure wave is formed and developed while taking the largest amplitude (profile 4). This development process of pressure waves can be referred to 'developing detonation' [2].

Figure 9 shows a part of the results in Case B, highlighting a generation mechanism for the first peak of pressure in Fig. 6. It is found that autoignition first occurs in a limited region in front of the propagating flame. This autoignition almost uniformly occurs, producing a new flame front at around $x = 3$ cm and

pressure waves with small amplitudes. Figure 10 presents a schematic of spatial distributions of equivalence ratio and its behaviors. As velocity fields are induced at the beginning by the ignition of a hot kernel, not only the flame but also an interface between two gases advect toward the right side, producing three regions in the domain: burnt gas, rich gas with $\phi = 1.2$, and lean gas with $\phi = 0.8$ regions, respectively. Therefore, autoignition first takes place in the region occupied with rich gas of $\phi = 1.2$ because of the faster ignition delay time compared to that with lean gas of $\phi = 0.8$.

Figure 11 shows sequential profiles of pressure and temperature, showing a process of the second peak generation. The autoignition occurs at the right wall in the region of $\phi = 0.8$ and a pressure wave is then generated, which is a similar process to that of Case A shown in Fig. 8. Eventually, the amplitude of the pressure wave becomes larger than that in Case A, resulting in the larger knocking intensity shown in Fig. 7.

Figure 12 shows sequential profiles of pressure and temperature in Case C. As shown in a schematic of Fig. 13, the three regions are generated similar to that in Case B. In Case C, a unique feature is that autoignition first occurs at the wall in the region of $\phi = 1.2$ according to the faster ignition delay time, producing a lower temperature spot with $\phi = 0.8$ in the middle part of the domain. The pressure wave generated at the right wall is developed in the region of $\phi = 1.2$ and just passes through the lower temperature spot with $\phi = 0.8$ without additional ignition event. Therefore, a single peak is only observed in Case C. The autoignition also occurs in the lower temperature spot in some time; but the pressure wave generated cannot be developed because there are no reactive gases in the domain.

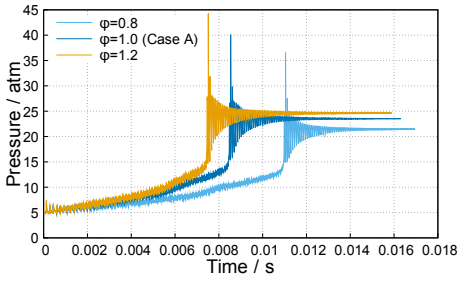


Figure 4: Transient histories of pressure at wall in uniform cases

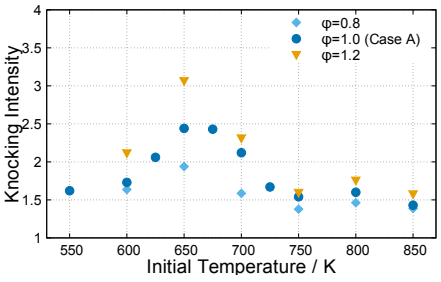


Figure 5: Knocking intensity against initial temperatures in uniform cases

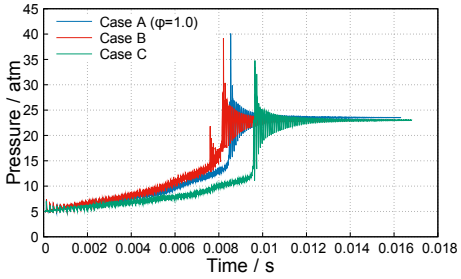


Figure 6: Transient histories of pressure at wall in non-uniform cases with Case A for comparison

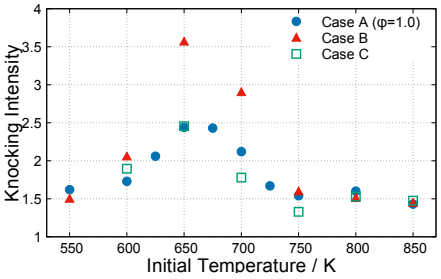


Figure 7: Knocking intensity against initial temperatures in non-uniform cases with Case A for comparison

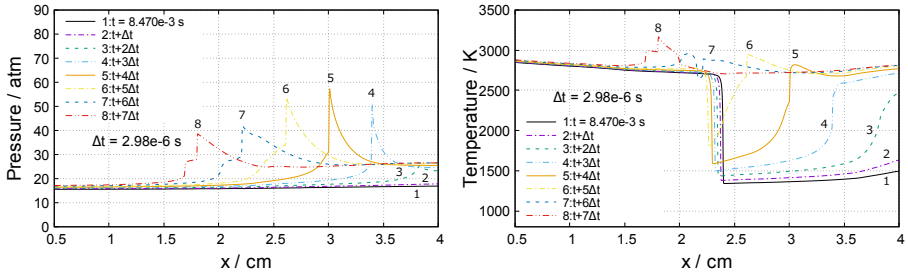


Figure 8: A temporal sequence of pressure and temperature profiles for an initial temperature of 650K in Case A (left: pressure; right: temperature)

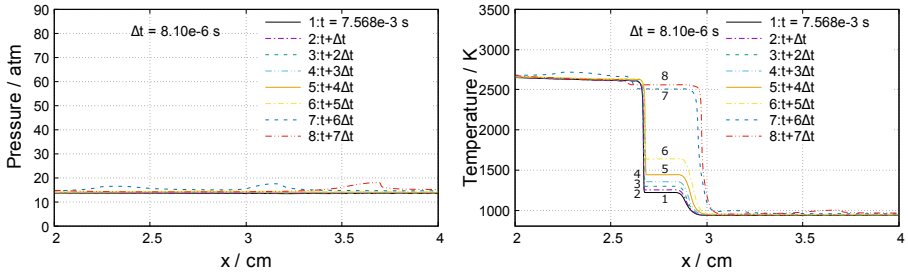


Figure 9: A temporal sequence of pressure and temperature profiles for an initial temperature of 650K in first autoignition of case B (left: pressure; right: temperature)

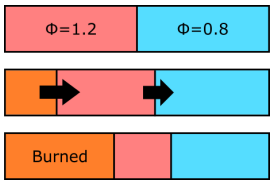


Figure 10: Schematic of the spatial distribution of equivalence ratio in Case B

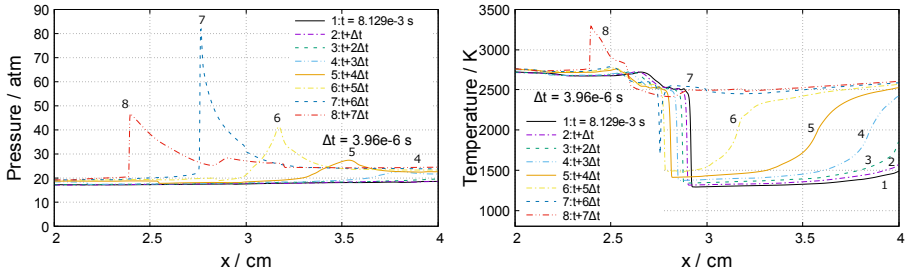


Figure 11: A temporal sequence of pressure and temperature profiles for an initial temperature of 650K in second autoignition of case B (left: pressure; right: temperature)

## 5 Conclusions

A simulation for knocking combustion has been performed to investigate the effects of fuel/air mixture distributions on the mechanisms of end-gas autoignition and pressure wave generation. In Case B, where the region initially consists of rich gas for the left side and lean gas for the right side, two autoignition events

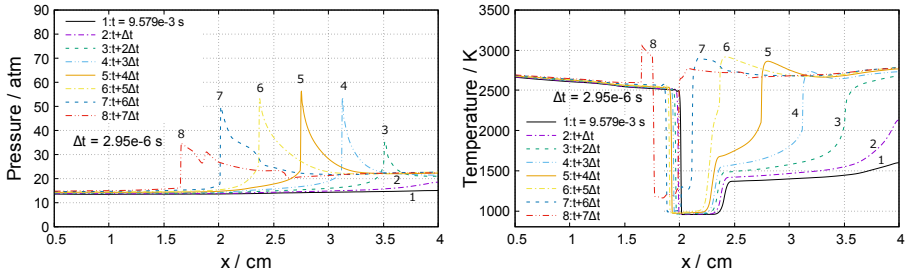


Figure 12: A temporal sequence of pressure and temperature profiles for an initial temperature of 650K in case C (left: pressure; right: temperature)

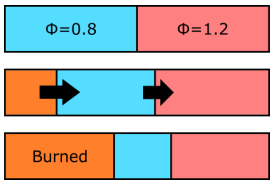


Figure 13: Schematic of the spatial distribution of equivalence ratio in Case C

are uniquely observed, generating two peaks in the pressure time histories. The first autoignition occurs in the rich region with $\phi = 1.2$ between the propagating flame and lean region with $\phi = 0.8$, followed by the second autoignition in the lean region with $\phi = 0.8$. The largest knocking intensity is thus produced in Case B. In Case C with the opposite distribution, a single peak in the pressure time histories is observed associated with the autoignition in the rich region with $\phi = 1.2$, which is a similar behavior to that with a uniform mixture case, Case A, demonstrating the importance of fuel/air mixture distributions on knocking phenomena.

## References

[1] X. Zhen, Y. Wang, S. Xu, Y. Zhu, C. Tao, T. Xu, and M. Song, "The engine knock analysis - An overview," *Applied Energy*, vol. 92, pp. 628–636, 2012.

[2] X. J. Gu, D. R. Emerson, and D. Bradley, "Modes of reaction front propagation from hot spots," *Combustion and Flame*, vol. 133, no. 1-2, pp. 63–74, 2003.

[3] P. Dai, Z. Chen, S. Chen, and Y. Ju, "Numerical experiments on reaction front propagation in n-heptane/air mixture with temperature gradient," *Proceedings of the Combustion Institute*, vol. 35, no. 3, pp. 3045–3052, 2015.

[4] H. Terashima and M. Koshi, "Mechanisms of strong pressure wave generation in end-gas autoignition during knocking combustion," *Combustion and Flame*, vol. 162, no. 5, pp. 1944–1956, 2015.

[5] A.Miyoshi, "KUCRS software library, available from the author. See the web," http://akrmys.com/KUCRS/.